

## Light Emission at a Metal-Insulator Contact under High Electric Fields

C. Paracchini

*Istituto di Fisica, Università di Parma, Parma, Italy*

(Received 12 April 1971).

Intrinsic luminescence at a metal-insulator contact has been observed in NaI, KI, and RbI single crystals with evaporated Au electrodes. The effect has been observed when a varying electric field ( $\gtrsim 10^4$  V/cm) is applied. The light emission is attributed to the recombination of the pairs created by impact ionization processes in a potential barrier near the contacts. Two mechanisms for the formation of the primary electrons are evidenced. A time dependence of the effect suggests the formation of space charges whose field opposes the external one. The experimental results suggest that only a few electrons among those accelerated by the internal field gain enough energy to produce the multiplication processes.

### I. INTRODUCTION

The light emitted from dielectric samples under high electric fields can give useful information about the injection and transport processes in insulators and semiconductors. This technique is particularly profitable in the materials where current measurements are difficult to make, that is, where the electrical conductivity is low and Ohmic injection is difficult, as in the wide-gap insulators. In such materials, the free carriers are obtained by field emission (Fowler-Nordheim, Schottky, or Poole-Frenkel) or by impact ionization. All these processes demand high electric fields, and the required value rises with the energy gap of the material. Alkali halides are unfavorable for that reason, but they also offer advantages: The emission wavelength is easily detected by high-gain photomultipliers, large-size single crystals are obtainable, and this makes the detecting of the emission zones easier. Moreover, samples with low impurity density can be easily grown.

Observations on such phenomena have been reported in only a few papers.<sup>1,2</sup> New theoretical models have been recently proposed for the interpretation of the phenomena at high electric fields in crystalline insulators, and these effects can be used for a more complete understanding of the processes involved. In particular, O'Dwyer has recently proposed new theories to explain the intrinsic electron breakdown in wide-gap insulators, and his models can be verified by observing the luminescence of the sample at high electric fields.<sup>3</sup>

In this work the electroluminescence obtained from an alkali-halide single crystal near a junction with a metal electrode is reported. The light emission has been observed with fields higher than  $10^4$  V/cm and only with time-varying applied voltage.

The luminescence is intrinsic, and since several studies were done on alkali halides using this phenomenon, its optical aspects can be easily compared

with the results reported in bibliography.<sup>4</sup> Alkali iodides are particularly useful because the intrinsic recombination is radiative at liquid-nitrogen temperature (LNT), while for other alkali halides, electrons and holes recombine through phonon processes down to much lower temperatures. Moreover alkali iodides have lower energy gap and higher electrical conductivity, thus making this kind of observation easier.

The effect has been observed in NaI, KI, and RbI at LNT. The results described in this paper deal mainly with KI. The results obtained with NaI and RbI will be presented when a particular aspect of the phenomenon is generalized or when the results seem more significant and evident than the results for KI.

### II. EXPERIMENTAL

The samples were cut in square slices ( $1 \times 1$  cm) about 0.5 mm thick. They were freshly cleaved from single crystals. KI crystals were grown in our laboratory in a  $N_2$  atmosphere by the Kyropoulos method; NaI and RbI crystals were supplied by Harshaw Chemical Company.

On one or both of the square faces a thin gold film was deposited in order to form a circular contact, the diameter of which (6 mm) was small enough compared with the size of the sample to avoid electrical discharges along the edges.

The specimens so prepared were placed in a carefully evacuated container ( $10^{-6}$  Torr) between two cylindrical copper electrodes with the same diameter as the gold contact. One electrode was in direct thermal contact with the liquid-nitrogen reservoir, in order to make all the measurements at 78 °K. To avoid the effects of thermal contraction, the crystal slices were sandwiched between the electrodes with the aid of a soft stainless-steel spring.

Most of the measurements were performed with only one electrode in contact with the sample. In such cases, the gold contact was deposited on one

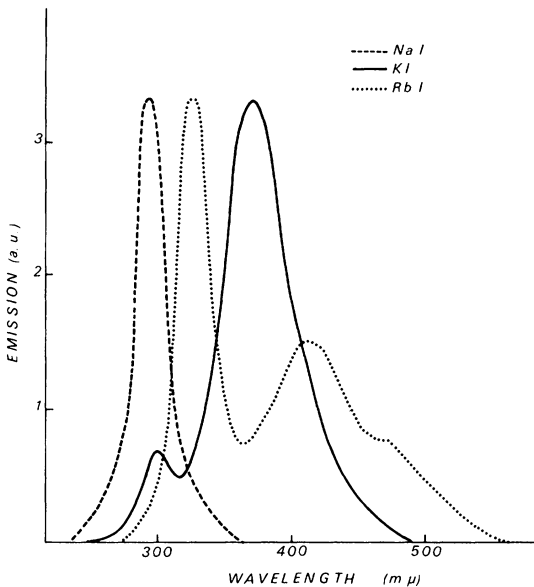


FIG. 1. Emission spectra obtained with NaI, KI, and RbI samples. Emission is normalized to the maximum of each curve.

side only; the other face was insulated from the copper electrode by means of a thin (0.02-mm) Teflon foil.

The emitted light was detected, in a direction perpendicular to the electric field, by means of a trialkali photomultiplier selected for low-noise level (EMI 9558 QA). Its spectral response ranges from 200 to 800  $m\mu$ . The phototube current signal was measured with an oscilloscope (Tektronix 7504), with a Boxcar integrator (PAR 160), or with a logarithmic amplifier (HP 7563A). The input impedance was always kept at  $10^5 \Omega$  in order to have a time constant lower than  $10^{-6}$  sec.

The emission spectra were obtained with a grating monochromator (Jarrel-Ash 82400). The time-integrated signal was measured in this case by means of a micromicroammeter (Keithley 414).

The electric field was provided by a function generator (Wavetek 116) or by a pulse generator (Chronetics PG 14). The excitation function was then amplified by a power amplifier followed by a step-up transformer. The evaluation and the waveform control of the high-voltage excitation was provided with a probe (Tektronix P6015) and the signal was sent to the oscilloscope for the comparison with the brightness waves. The frequency of the periodic excitation ranges from 50 to 3000 Hz. The rise rate of the steps is about  $10^4$  V/msec.

### III. RESULTS

The emission spectrum for all the three cases confirms that the observed luminescence is due to the recombination of free electrons with self-

trapped holes ( $V_k$  centers). Figure 1 shows the spectra obtained for the three alkali iodides examined. In all cases the observed bands coincide with those of the intrinsic recombination obtained from photoluminescence measurements by other authors.<sup>4</sup>

In the RbI case, besides the bands at 320 and 430  $m\mu$  ascribable to the intrinsic recombination, other emissions at longer wavelengths are observed. These bands are probably due to impurities photoexcited by the intrinsic luminescence in a way similar to that already reported for KI samples doped with silver.<sup>5</sup>

The spectra of the luminescence confirm that the light is emitted from the crystal and that during the process free pairs of carriers are formed. The low mobility of the holes causes them to be trapped immediately.

The intrinsic luminescence lifetime, as reported by other authors, is about  $10^{-6}$  sec for the 380- $m\mu$  emission of KI.<sup>4</sup> This is one of the longest intrinsic luminescence lifetimes in alkali-halide crystals. Measurements described later revealed that the effect after a step excitation fades out in few milliseconds. The self-trapping of the holes and their recombination with the free electrons takes place in a time much shorter than that of the decay of the observed effect. The light emitted is then proportional to the number of pairs created per unit time.

The luminescence takes place only when the excitation voltage varies in time. The light emission has been observed with fields larger than  $10^4$  V/cm. The brightness waves are compared with those due to sinusoidal excitation in Fig. 2. The upper picture is for a NaI sample, the lower for KI. The effect obtained with RbI is similar to that with KI.

The photographs of Fig. 2 are obtained with only one electrode in contact with the crystal. It is evident that the light is emitted approximately when the metal contact reaches both the positive and the negative maxima. The brightness waves lead the voltage by approximately  $\frac{1}{4}\pi$ .

The frequency of the light emission is twice that of the excitation. This fact shows that the effect is not due to alternate emission of electrons and holes from the metal contact. In such a case the light peaks would appear only at the negative maxima, and no phase shift would take place between the brightness and the voltage waves. It must be remembered, in fact, that it is the electrons that recombine with the trapped holes and not vice versa. The carrier injection from the metal contacts is in any case necessary, because no light emission is obtained when both the electrodes are insulated from the sample by means of thin Teflon foils. According to the alternative hypothesis, only one type of carrier is injected from the electrode and the pairs are subsequently created by

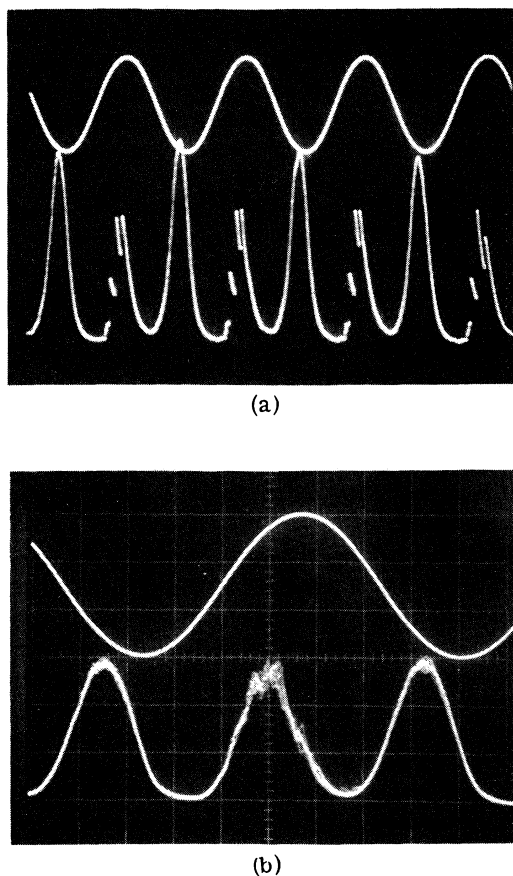


FIG. 2. Voltage and brightness waves for NaI (a) and KI (b) samples. Frequency: 300 Hz. Maximum applied field:  $7.5 \times 10^4$  V/cm. Voltage polarity is referred to the electrode in contact with the sample.

impact ionization. On account of the low mobility of the holes, the injected carriers must be electrons; holes are formed by ionizing electrons from the valence band.

These hot-electron processes can take place only near the metal contact, where a potential barrier is formed. Figure 3 shows a KI sample under excitations; it is evident that the effect is limited to a thin zone near the contact.

The brightness waves obtained with rectified sinusoidal and square excitations are shown in Fig. 4. In these cases too, the metal contact is negatively biased. The photographs show two light pulses: The first appears when the applied field is growing, the second on its removal. Two different mechanisms for the production of the primary electrons are then required. In this connection the following model is proposed.

Field emission from the metal contact takes place when it is negatively biased. The injected electrons are accelerated by the field in the potential barrier at the metal-insulators junction. In this way they

gain energy enough to create new pairs, which recombine radiatively in part. Beyond the barrier the injected electrons reach a low-field zone, where they become trapped in shallow levels. These trapped electrons build up a space charge whose field quenches that externally applied. As long as the external voltage remains constant, there is equilibrium; when the applied field is reduced, the space-charge field prevails: It ionizes some of the shallow traps, and accelerates the freed electrons up to the ionizing energy again.

It is supposed that the space charge of the injected electrons reduces the external field exponentially, as during the charging of a capacitor. In this case the internal field leads the external one, in accordance with what appears in Figs. 2 and 4.

The phase-shift-of-light peaks with respect to the applied-voltage maxima in Fig. 4 give an approximate measure of the time constant  $\tau$ , which is found to be between 1.5 and 3 msec.

The proposed model is qualitatively confirmed by the NaI brightness waves (Fig. 2). The difference between the successive light peaks is particularly evident in this case: When the metal contact is negatively biased, the light is emitted smoothly; in the other case abrupt rises of light emission are evident. Field emission from shallow traps may account for this effect, and it may explain also the abrupt rises in the integrated brightness plotted vs the amplitude of excitation, as obtained for NaI. Though for KI and RbI the evidence is not so striking, probably the same effect takes place.

The proposed model may be confirmed also by the temporary light increase observed after the illumination of the sample with white or uv light. This effect is particularly evident when x-irradiated specimens are used. In these cases the trap concentration is higher, and the light excitation fills



FIG. 3. Photograph of KI sample excited by an alternating electric field. Light emission is localized near the gold contact deposited on the upper face of the crystal. Applied field:  $6 \times 10^4$  V/cm. Frequency: 300 Hz.

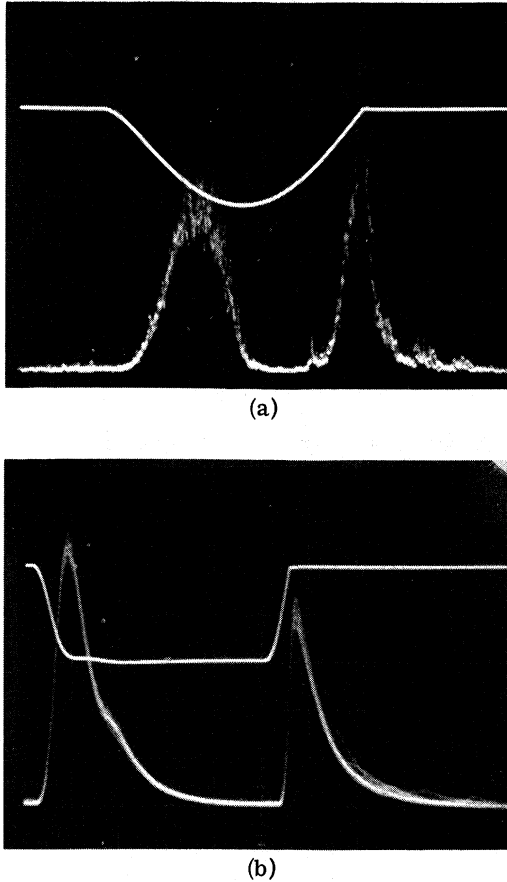


FIG. 4. Voltage and brightness waves for a KI sample. Excitation pulses are obtained with a rectified sinusoidal and a square wave. Maximum applied field:  $4 \times 10^4$  V/cm.

the traps that are later ionized by the electric field.

As far as two mechanisms are involved, the study of the brightness integrated over a half-cycle is not so profitable. The instantaneous correlation between light emission and excitation is then preferred.

#### IV. DISCUSSION

This discussion deals only with the part of the effect which takes place when the metal contact is negatively biased with increasing voltage values. In this case, the primary electrons are field emitted by tunneling from the contact into the potential barrier; the number of injected electrons can be assumed much smaller than the number of pairs created.

The electron-hole pairs recombine partly radiatively, partly through radiationless transitions. The efficiency of the radiative recombination is temperature dependent.<sup>4</sup> Keeping the sample at constant temperature, the emitted light  $L$  is proportional to the number of pairs created.

If  $\alpha$  is the ionization rate (that is, the average

number of pairs created by a single electron traveling a unit distance in the direction of the electric field) and  $v$  is the electron drift velocity, then the number of photons emitted per unit time  $dn/dt$  is

$$\frac{dn}{dt} = \frac{dn}{ds} \frac{ds}{dt} = \alpha(F)v(F). \quad (1)$$

Both  $\alpha$  and  $v$  are functions of the internal local field  $F$ .

The relation between the external applied field  $E$  and  $F$  depends on the type of the potential barrier which appears at the boundary between the metal contact and the bulk of the insulator. High-resistivity materials have a free-carrier density  $n$  lower than that of the trapped carriers,  $n_t$ . For such materials, when the traps are differently distributed in energy, an exponential barrier is formed,<sup>6</sup> and  $F$  is proportional to  $E$ . Schottky barriers, with  $F \sim \sqrt{E}$ , are, on the contrary, more common in low-resistivity materials. These barriers appear when  $n_t < n$  or when there is one single-trap level.

In the present case, in stationary conditions,  $F$  may be taken proportional to  $E$ . The phase shift between response and excitation, as shown in Figs. 2 and 4, shows that the effect is not stationary. It must be remembered, in this connection, that the light output is a monotonic function of the excitation amplitude.

Because of the formation of a space charge, the internal field  $F$  decreases exponentially in time with respect to the applied field  $E$ . This same reason explains the absence of the effect when a constant field is applied to the sample.

After a time  $t'$  from the beginning of the excitation one has

$$F(t') \sim \int_0^{t'} \frac{dE(t)}{dt} \exp\left(-\frac{t-t'}{\tau}\right) dt. \quad (2)$$

If  $E$  increases linearly with time ( $E = \beta t$ ), expression (2) becomes

$$F(t') \sim \beta(1 - e^{-t'/\tau}) = E(\tau/t')(1 - e^{-t'/\tau}). \quad (3)$$

From (3) it is possible to know the value of  $F$  at every instant as a function of  $E$  and  $t'$ . The value of  $\tau$  is obtained by using expression (2) to correlate the phase difference between the light and the voltage maxima in several photographs like that shown in the upper part of Fig. 4. In this case  $E(t) = \sin \omega t$ , and  $F(t)$  has a maximum when an implicit function  $f(\tau, \omega, t) = 0$ . Knowing  $\omega$ , and taking  $t$  as the time elapsed from the beginning of the sinusoidal excitation to the maximum of light output, it is possible to deduce  $\tau$ . For this purpose, the maximum of the internal field is supposed to coincide with the maximum of the effect. Such measurements do not give a precise value of  $\tau$ , and the results obtained range from 1.5 to 3 msec. The most common value,  $\tau = 2$  msec, is chosen to relate  $E$  and  $F$

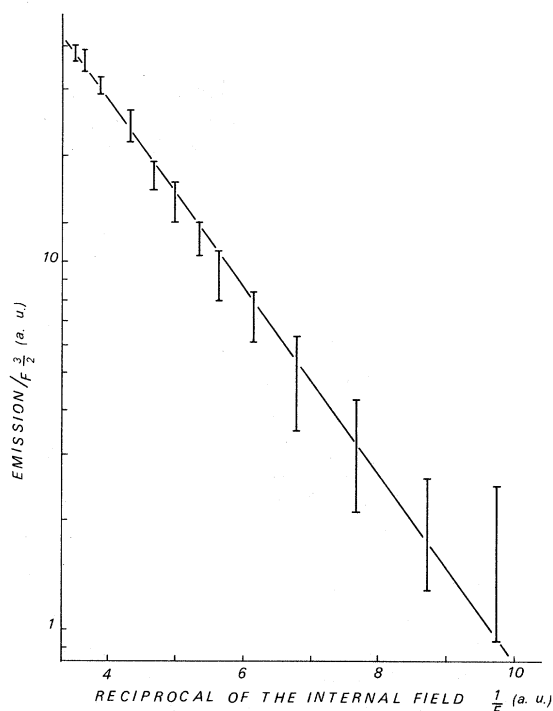


FIG. 5. Plot of  $L = BF^{3/2} e^{-b/F}$ . Values of  $L$  are obtained at successive instants with a negative excitation linearly increasing ( $\beta = 4$  kV/msec). Values of  $F$  are obtained from Eq. (3) with  $\tau = 2$  msec.

through Eq. (3). However, taking any values of  $\tau$  between 1.5 and 3 msec would not alter the following considerations.

If the internal field  $F > c/\mu_0$  (where  $c$  is the speed of the longitudinal acoustic waves and  $\mu_0$  is the electron mobility at low fields), one has  $v \sim (\mu_0 F c)^{1/2}$ .<sup>7</sup> In the present case,  $c/\mu_0 \approx 10^3$  V/cm, and the effect has been observed for  $E > 10^4$  V/cm, where  $v \sim \sqrt{F}$ .

Several authors have treated the acceleration of electrons up to ionizing energies in insulators where the carrier density is so low that electron-electron interactions can be ignored. Basically there are two solutions: The first is valid when the average energy of the electrons,  $\bar{\epsilon}$ , is higher than the ionization energy  $\epsilon_i$ , and the second when only a few electrons have energy high enough to give rise to impact ionization ( $\bar{\epsilon} < \epsilon_i$ ).<sup>8</sup> Accordingly, one has

$$\alpha \sim e^{-a/F^2} \quad \text{if } \bar{\epsilon} > \epsilon_i, \quad \alpha \sim F e^{-b/F} \quad \text{if } \bar{\epsilon} < \epsilon_i,$$

where  $a$  and  $b$  are independent of  $E$ . Then  $L$  is proportional to

$$F^{1/2} e^{-a/F^2} \quad \text{if } \bar{\epsilon} > \epsilon_i$$

or to

$$F^{3/2} e^{-b/F} \quad \text{if } \bar{\epsilon} < \epsilon_i.$$

Figure 5 shows  $\ln(L/F^{3/2})$  plotted as a function of  $1/F$ . The values of  $L$  are obtained applying to the contact a negative, linearly increasing voltage with  $\beta = 4$  kV/msec. The values of  $E$  are corrected at successive instants with Eq. (3) in order to obtain the internal field  $E$ . Figure 6 shows the same experimental values of  $L$  plotted as  $\ln(L/F^{1/2})$  vs  $1/F^2$ . According to the above-mentioned theories the average energy of the electrons, in the case examined, is lower than that required for impact ionization, and the pair creation is affected only by the more energetic electrons.<sup>8</sup>

## V. CONCLUSIONS

The observed phenomenon can be explained by considering the formation of a potential barrier at the metal-insulator junction where the local field is greatly enhanced. In this region the primary electrons are accelerated up to impact ionization energy and new pairs of carriers are formed.

According to the polarity of the metal contact, the primary electrons are injected from the electrons or they are field emitted from shallow traps.

The acceleration of the electrons in the barrier takes place as if the local fields were proportional to that externally applied (Rose-type barrier).

The velocity distribution function of the electrons is not spherically symmetric, and only few of them

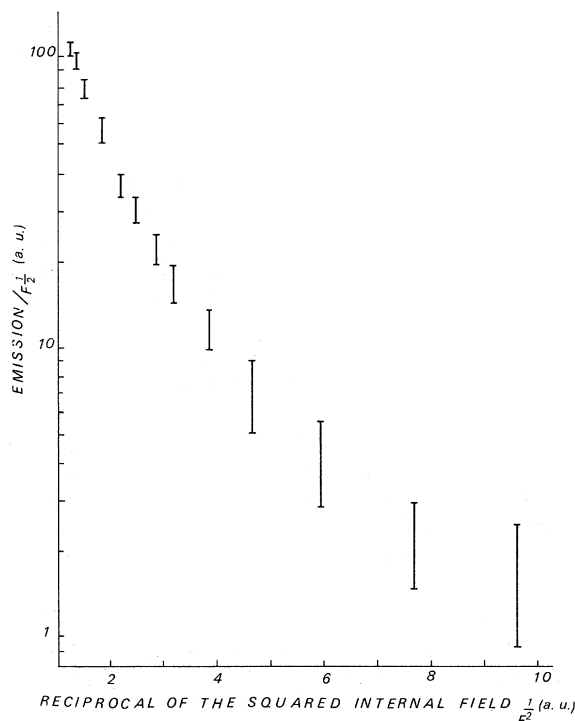


FIG. 6. Plot of  $L = AF^{1/2} e^{-a/F}$ . Values of  $L$  and  $F$  are those used in Fig. 5.

have energy enough to give rise to impact ionization.

The movement of the carriers in the electric field creates a space charge whose field opposes the external one, thus reducing it exponentially with a time constant  $\tau = 1.5\text{--}3$  msec. When the applied voltage is removed, the space-charge field gives

rise to the processes leading to the effect.

#### ACKNOWLEDGMENTS

The author is grateful to Professor R. Fieschi and to Professor E. Fatuzzo for useful discussions. The Gruppo Nazionale della Materia (GNSM) has supported this work.

<sup>1</sup>S. Unger and K. Teegarden, *Phys. Rev. Letters* **19**, 1229 (1967).

<sup>2</sup>R. Cooper and C. T. Elliott, *J. Phys. D* **1**, 121 (1968).

<sup>3</sup>J. J. O'Dwyer, *J. Appl. Phys.* **39**, 4356 (1968); **40**, 3887 (1969).

<sup>4</sup>See, for example, K. Teegarden, in *Luminescence of Inorganic Solids*, edited by P. Goldberg (Academic,

New York, 1966).

<sup>5</sup>C. Paracchini and G. Schianchi, *Solid State Commun.* **8**, 1769 (1970).

<sup>6</sup>A. Rose, *Helv. Phys. Acta* **29**, 199 (1956).

<sup>7</sup>W. Shockley, *Bell System Tech. J.* **30**, 990 (1951).

<sup>8</sup>A. G. Chynoweth, in *Semiconductors and Semimetals*, Vol. 4, edited by R. K. Willardson and A. C. Beer (Academic, New York, 1968), pp. 268–286.

## Influence of Magnetic Ordering on a Phonon Resonant Mode in Chlorine-Doped $\text{MnF}_2$ †

D. Bäuerle\*

*Laboratory of Atomic and Solid State Physics, Cornell University, Ithaca, New York 14850*

(Received 21 May 1971)

The far-infrared absorption spectra of chlorine-doped  $\text{MnF}_2$  show a strong phonon resonant mode at  $35.79 \pm 0.03 \text{ cm}^{-1}$  ( $1.2^\circ\text{K}$ ). The electric vector of this mode is polarized perpendicular to the  $c$  axis of the crystal. In order to study the influence of magnetic ordering on this mode, the center frequency and half-width were measured as a function of temperature from  $1.2^\circ\text{K}$  through the Néel point up to  $100^\circ\text{K}$ . The resonant frequency increases monotonically with temperature. An additional shift was observed at the onset of magnetic ordering, and was accompanied by additional broadening of the line. These anomalies are explained by considering magnetoelastic effects.

### I. INTRODUCTION

In  $\text{MnF}_2$  many studies have been done in connection with optical absorption associated with magnetic impurities. However, in this substance little is known about phonon impurity modes and nothing about their interaction with the magnetic lattice.

The first measurements on the far-infrared vibrational absorption of  $\text{Eu}^{2+}$  and  $\text{Tm}^{3+}$  in  $\text{MnF}_2$  were done by Alexander and Sievers.<sup>1</sup> To our knowledge, in  $\text{MnF}_2$  no phonon modes due to anion substitutes are known.

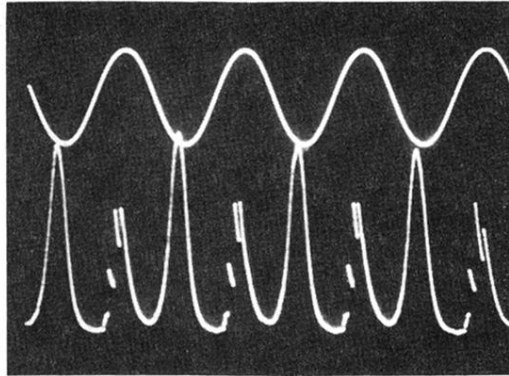
In this paper we report on a phonon resonant mode which we found in  $\text{Cl}^-$ -doped  $\text{MnF}_2$ .<sup>2</sup> The influence of magnetic ordering on this mode was studied by measuring the center frequency and half-width of the resonance as a function of temperature from  $1.2^\circ\text{K}$  through the Néel point ( $T_N = 67.3^\circ\text{K}$ ) up to  $100^\circ\text{K}$ .

### II. EXPERIMENTAL

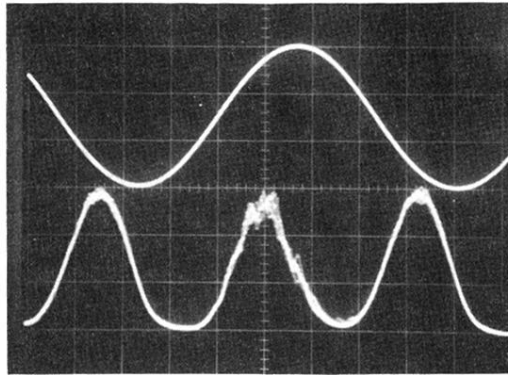
Single crystals of pure and  $\text{Cl}^-$ -doped  $\text{MnF}_2$  were oriented by the Laue back-reflection method within

a few tenths of a degree and cut perpendicular and parallel to the  $c$  axis of the crystal. The far-infrared absorption spectra of pure and doped samples were measured for both polarizations in the region from 3 to  $90 \text{ cm}^{-1}$ . Between 3 and  $50 \text{ cm}^{-1}$  a lamellar interferometer was used with a  $\text{He}^3$  cooled bolometer detector; for the higher-energy region, a Michelson interferometer was used with a  $1.2^\circ\text{K}$  bolometer. The maximal instrumental resolution was about  $0.1 \text{ cm}^{-1}$  in both cases.

The most remarkable feature in the absorption spectra of the doped samples is a strong absorption line at  $35.79 \pm 0.03 \text{ cm}^{-1}$  ( $1.2^\circ\text{K}$ ). The dipole moment in this mode is perpendicular to the  $c$  axis of the crystal. The impurity-induced absorption coefficient is shown in Fig. 1 for different sample temperatures. The integrated absorption of the line,  $\int \alpha(\omega) d\omega$ , decreases from  $1.2$  to  $100^\circ\text{K}$  by  $(16 \pm 12)\%$ . The error is caused by uncertainty in determining the absolute baseline of the absorption. At  $1.2^\circ\text{K}$  no change in center frequency was observed when the doping with  $\text{Cl}^-$  in the melt varied between 0.5 and 2%.<sup>3</sup>



(a)



(b)

FIG. 2. Voltage and brightness waves for NaI (a) and KI (b) samples. Frequency: 300 Hz. Maximum applied field:  $7.5 \times 10^4$  V/cm. Voltage polarity is referred to the electrode in contact with the sample.

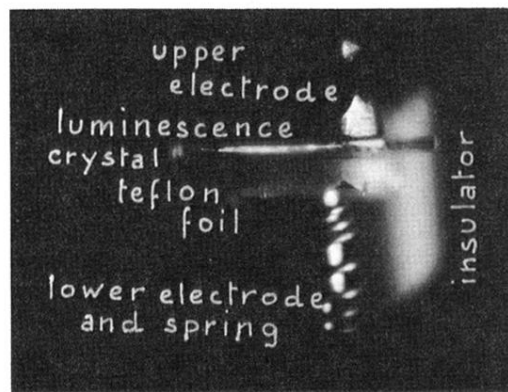
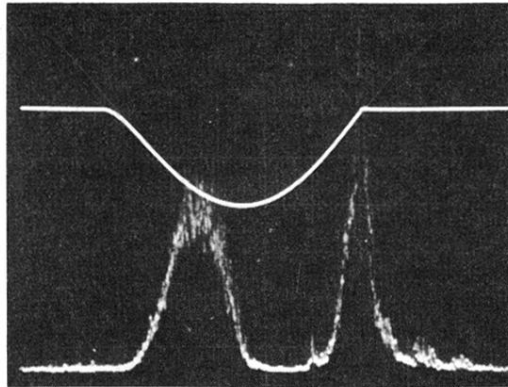
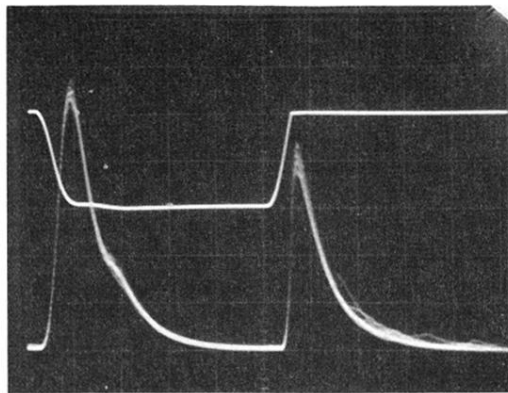


FIG. 3. Photograph of KI sample excited by an alternating electric field. Light emission is localized near the gold contact deposited on the upper face of the crystal. Applied field:  $6 \times 10^4$  V/cm. Frequency: 300 Hz.





(a)



(b)

FIG. 4. Voltage and brightness waves for a KI sample. Excitation pulses are obtained with a rectified sinusoidal and a square wave. Maximum applied field:  $4 \times 10^4$  V/cm.